BL-16A/2021G501

Evidence of Variations of Magnetic Properties of Vanadium Doped $CaRuO_3$ using X-Ray Magnetic Circular Dichroism

R. DAWN[1], M.ZZAMAN[1], V K. VERMA[2], K. KUMAR[3], A. PRAMANIK[4], A. KANDASAMI[5] and K. AMEMIYA[6], V. R. SINGH[1]*

[1]Department of Physics, Central University of South Bihar, Gaya 824236

[2]Department of Physics, VIT-AP University, Beside AP Secretariat, Near Vijayawada, Amaravati 522237 A.P. India

[3]Department of Physics, Ranchi University, Ranchi 834008, India

[4]School of Physical Sciences, Jawaharlal Nehru University, New Delhi 110067, India

[5]Department of Physics & Centre for Interdisciplinary Research, University of Petroleum and Energy Studies (UPES) Dehradun, Uttarakhand 248007, India

[6]Photon Factory, IMSS, High Energy Accelerator Research Organization, Tsukuba, Ibaraki 305-0801, Japan

1. INTRODUCTION: The *d*-band metal oxides are renowned among materials due to the complexity of their phase diagram that exhibits a formidable array of close and almost overlapping transitions between metallic, insulating, magnetic, and even for superconducting phases [1]. After a long era of intensive study, a full theoretical understanding of such puzzled phase diagram still remains unsolved. In a typical scenario, one starts from an insulating, antiferromagnetically ordered state when the d-band is half-filled or nearly so. This is a classic example of a Mott insulator in which the single occupancy of each lattice site prevents free motion of the charge. Moving away from the half-filled situation (through chemical substitutions or doping, as for example) the charge eventually unfreezes, leading to a metallic phase with striking non-Fermi liquid properties and in some cases to a superconducting phase. In parallel to this, the nature of magnetic correlation changes dramatically from predominantly antiferromagnetic (superexchange-like) in the Mott-localized phase to predominantly ferromagnetic (Hund-like) in the delocalized metallic phase. Recent advances in the atomic-scale control of transition metal oxide interfaces offer new opportunities for the manipulation of strongly correlated electron systems with a growing awareness of the wealth of microscopic phenomena that need to be understood in order to arrive at a quantitative description of the electronic state at oxide interfaces. Magnetic fluctuations accompanying with insulator-to-metal transition and the associated quantum magnetic critical behaviour are often considered to be the underlying physics behind the unconventional superconductivity in magnetic materials of the strongly correlated electrons origin [2,3]. Despite the heavy interest in this topic, the situation is still not well understood.

Motivated by the above considerations, we have undertaken a careful experimental study of the interplay between the insulator to metal transition and magnetism in the perovskites $Ca(Ru_{1-0.05}V_{0.05})O_3$. These compounds crystallize in an orthorhombic lattice configuration with end members, $CaRuO_3$ (x= 0) and $CaVO_3$ (x= 1), being an anomalous metal and a Mott insulator, respectively [1,4].

Although the static magnetic characteristics of $CaRuO_3$ is still a matter of debate– whether it is a paramagnet or on the verge of the ferromagnetic instability, strong magnetic fluctuations of ferromagnetic origin were detected in the NMR measurements [3]. Recent experimental studies suggest a coexistence of the quantum magnetic fluctuations and non-Fermi liquid behaviour for $T \leq$ 25K, albeit no magnetic order is detected to the lowest measurement temperature [1]. Y Shirako *et al* reported that an inflection point near 270 K implies some transition, e. g. establishment of a long-range magnetic order below the temperature while the isothermal magnetization clearly indicates the absence of spontaneous magnetization over the temperature range which strongly suggest that $CaRuO_3$ possess antiferromagnetic interaction and its Néel temperature, T_N, is around 270 K [2].

2. EXPERIMENT: The high purity polycrystalline samples of $Ca(Ru_{1-0.05}V_{0.05})O_3$ were synthesized by conventional solid-state reaction method using ultra-pure ingredients of V_2O_5, RuO_2 and $CaCO_3$. Starting materials were mixed in stoichiometric composition, with five percent extra RuO_2 to compensate for their rapid evaporation (in Ru-doped perovskites),

pelletized and sintered at 950° C for three days. The furnace cooled samples were grinded, pelletized and sintered at 1000° C for another three days. Resulting samples were characterized using Rigaku Smart Lab powder X-ray diffractometer, confirming the single phase of material. X-ray spectroscopy, scattering, and imaging experiments were performed at the variable-polarization soft x-ray beam-line BL-16A of the Photon Factory (KEK, Japan). Experimental geometry of soft x-ray absorption (XAS) and x-ray magnetic circular dichroism (XMCD) experiments are shown in Fig. 1 and 2. The sample was placed in the vacuum chamber with a pressure of 10^{-9} Torr equipped with a 5 T superconducting magnet. XAS and XMCD signals were measured at ±0.1T, ±1T and ±2T varying magnetic-fields (only the data of ±2T has been produced here) with right and left circularly polarized (RCP and LCP) x-rays having an energy resolution of 0.1 eV using the bulk-sensitive total fluorescence yield (TFY) method near Ru $M_{4,5}$ and V $L_{2,3}$ absorption edges with right and left circularly polarized (RCP and LCP) x-rays.

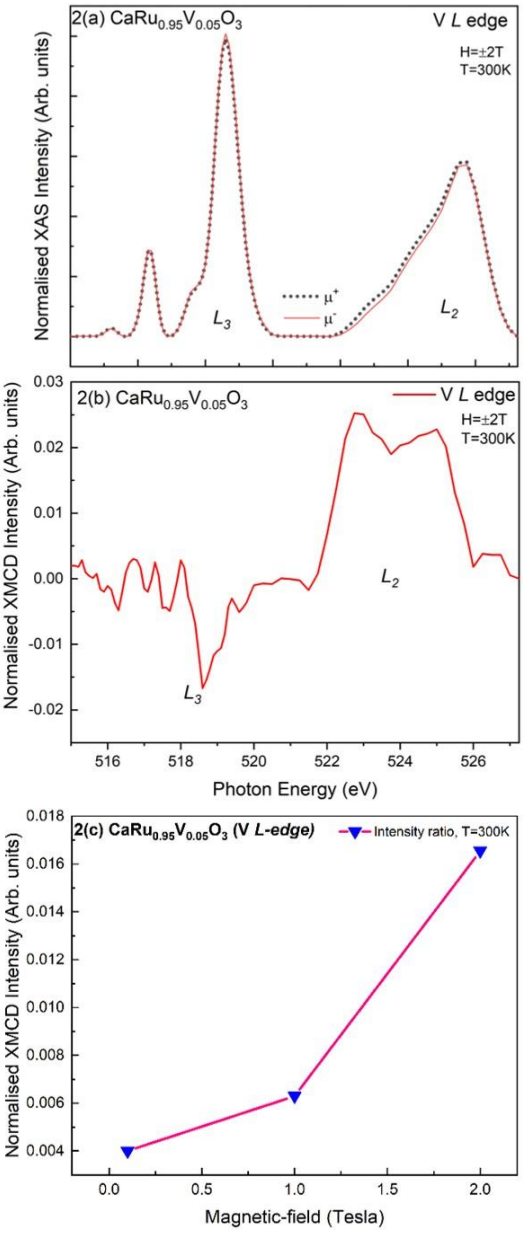

Fig 1(a) Normalised XAS spectra and Fig 1(b) Normalised XMCD spectra of Ru M4,5 site. Fig 1(c) XMCD/XAS Intensity ratio w.r.t. applied magnetic-field ±0.1T, ±1.0T and ±2.0T .

3.RESULTS AND DISCUSSIONS: The XAS spectra obtained with applied magnetic fields of

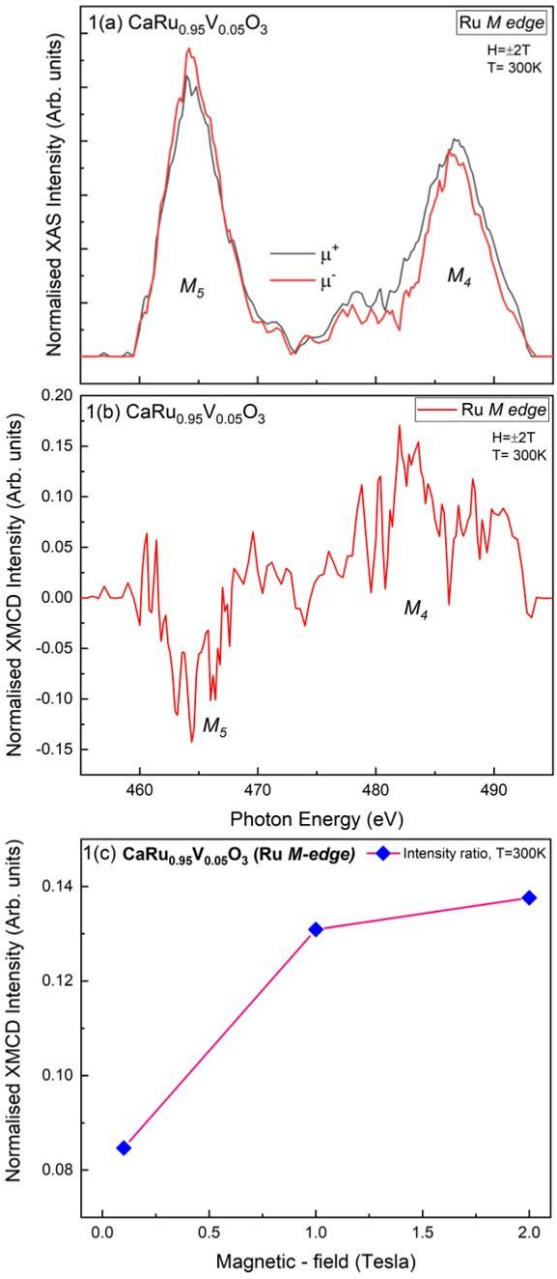

Fig 2(a) Normalised XAS spectra and Fig 2(b) Normalised XMCD spectra of V L2,3 site. Fig 2(c) XMCD/XAS Intensity ratio w.r.t. applied magnetic-field ±0.1T, ±1.0T and ±2.0T .

+2.0 and -2.0 T are denoted by μ^+ and μ^- which represent left and right circularly polarized light, respectively as shown in Fig 1(a) and 2(a). The

XMCD spectrum was recorded by taking a difference between the XAS spectra with negative and positive helicity of the circular polarized light. Ru and V both shows a tendency of multiplet structure at the M_5 and M_4, and L_3 and L_2 absorption edges, respectively. Well-resolved peaks at the absorption maxima at E = 464.54 eV and 468.64 eV at the M_5 and M_4 edges, respectively are clearly observable. This verifies that the fine structures of Ru *3d* → *4f* transition should result from the localization of Ru *4f* electrons rather than the oxidation of the material. V, on the other hand, have multiplet absorption peaks found at L_3 edges. The L_3 peak with absorption energy, E = 518.61 eV arrives with a satellite peak at 516.34 eV and a pre-peak region at 517.58 eV; whereas, L_2 shows a singlet peak at 525.68 eV. Such results implies that unlike Ru-site, V *2p* → *3d* transition is non-localised and infuses oxidation of the material. XMCD signal measured in a magnetic field of B =2.0 T (as produced here) for Ru $M_{4,5}$ and V $L_{2,3}$ is shown in Fig.1(b) and Fig.2(b), respectively. The XMCD feature of Ru $M_{4,5}$ and V $L_{2,3}$ is anti-parallel to each other which predicts that substitution of V in the place of Ru introduces an contrast effect in the mother-material $CaRuO_3$. The XMCD/XAS intensity ratio w.r.t. the variable magnetic field with ±0.1T, ±1.0T and ±2.0T are shown in Fig 1(c) for Ru-edges and in Fig 2(c) for V-edges. This result is quite relatable with the XMCD graphs. Fig 1(c) exhibits that the intensity ratio of XMCD/XAS is increasing with increasing magnetic-field; as same as Fig 2(c). This phenomenon suggests that after the doping of V at Ru-site, magnetic anisotropy gets increased which indicates an increase in ferromagnetism of the NPs. Although we do not have direct evidence of the ferromagnetic character of the fluctuation in x= 1 composition, it is justifiable to suggest that the data becomes negative, suggesting a tendency towards ferromagnetism arising a metallic feature of $CaVO_3$ at room temperature.

ACKNOWLEDGEMENTS: The experiment at the Photon Factory was approved by the Program Advisory Committee (Proposal Nos. 2021G501.

References:

[1] J. Gunasekera, L. Harriger, A. Dahal, T. Heitmann, G. Vignale & D. K. Singh, Scientific Reports **5**, 18047 (2016).

[2] Y. Shirako, H. Satsukawa, H. Kojitani, T. Katsumata, M. Yoshida, Y. Inaguma, K. Hiraki, T. Takahashi, K. Yamaura, E. T. Muromachi & M. Akaogi, J. Phys.: Conf. Ser. **215** 012038 (2010).

[3] J. W. Freeland, J. Chakhalian, A. V. Boris, J.-M. Tonnerre, J. J. Kavich, P. Yordanov, S. Grenier, P. Zschack, E. Karapetrova, P. Popovich, H. N. Lee, & B. Keimer, Physical Review B **81**, 094414 (2010).

[4] M. Gu, J. Laverock, B. Chen, K. E. Smith, S. A. Wolf & Jiwei Lu, Journal of Applied Physics **113**, 133704 (2013).

*Electronic Email: vijayraj@cusb.ac.in